

Durham Research Online

Deposited in DRO:

21 September 2017

Version of attached file:

Published Version

Peer-review status of attached file:

Peer-reviewed

Citation for published item:

Rapisarda, Valentina and Malashchuk, Igor and Asamaowei, Inemo E. and Poterlowicz, Krzysztof and Fessing, Michael Y. and Sharov, Andrey A. and Karakesisoglou, Iakowos and Botchkarev, Vladimir A. and Mardaryev, Andrei (2017) 'p63 transcription factor regulates nuclear shape and expression of nuclear envelope-associated genes in epidermal keratinocytes.', *Journal of investigative dermatology.*, 137 (10). pp. 2157-2167.

Further information on publisher's website:

<https://doi.org/10.1016/j.jid.2017.05.013>

Publisher's copyright statement:

This article is available under the terms of the Creative Commons Attribution License (CC BY). You may copy and distribute the article, create extracts, abstracts and new works from the article, alter and revise the article, text or data mine the article and otherwise reuse the article commercially (including reuse and/or resale of the article) without permission from Elsevier. You must give appropriate credit to the original work, together with a link to the formal publication through the relevant DOI and a link to the Creative Commons user license above. You must indicate if any changes are made but not in any way that suggests the licensor endorses you or your use of the work.

Additional information:

Use policy

The full-text may be used and/or reproduced, and given to third parties in any format or medium, without prior permission or charge, for personal research or study, educational, or not-for-profit purposes provided that:

- a full bibliographic reference is made to the original source
- a [link](#) is made to the metadata record in DRO
- the full-text is not changed in any way

The full-text must not be sold in any format or medium without the formal permission of the copyright holders.

Please consult the [full DRO policy](#) for further details.



JID Open

p63 Transcription Factor Regulates Nuclear Shape and Expression of Nuclear Envelope-Associated Genes in Epidermal Keratinocytes

Valentina Rapisarda^{1,4,5}, Igor Malashchuk^{1,5}, Inemo E. Asamaowei¹, Krzysztof Poterlowicz¹, Michael Y. Fessing¹, Andrey A. Sharov², Iakowos Karakesisoglou³, Vladimir A. Botchkarev^{1,2} and Andrei Mardaryev¹

The maintenance of a proper nuclear architecture and three-dimensional organization of the genes, enhancer elements, and transcription machinery plays an essential role in tissue development and regeneration. Here we show that in the developing skin, epidermal progenitor cells of mice lacking p63 transcription factor display alterations in the nuclear shape accompanied by a marked decrease in expression of several nuclear envelope-associated components (Lamin B1, Lamin A/C, Sun1, Nesprin-3, Plectin) compared with controls. Furthermore, chromatin immunoprecipitation-quantitative PCR assay showed enrichment of p63 on *Sun1*, *Syne3*, and *Plec* promoters, suggesting them as p63 targets. Alterations in the nuclei shape and expression of nuclear envelope-associated proteins were accompanied by altered distribution patterns of the repressive histone marks trimethylation on lysine 27 of histone H3, trimethylation on lysine 9 of histone H3, and heterochromatin protein 1-alpha in p63-null keratinocytes. These changes were also accompanied by downregulation of the transcriptional activity and relocation of the keratinocyte-specific gene loci away from the sites of active transcription toward the heterochromatin-enriched repressive nuclear compartments in p63-null cells. These data demonstrate functional links between the nuclear envelope organization, chromatin architecture, and gene expression in keratinocytes and suggest nuclear envelope-associated genes as important targets mediating p63-regulated gene expression program in the epidermis.

Journal of Investigative Dermatology (2017) 137, 2157–2167; doi:10.1016/j.jid.2017.05.013

INTRODUCTION

Epidermis is a stratified self-renewing epithelium, in which lineage-committed progenitor cells residing in the basal layer proliferate and differentiate into cells of the suprabasal layers to form epidermal barrier (Blanpain and Fuchs, 2009; Fuchs, 2007).

Terminal differentiation in epidermal keratinocytes is accompanied by structural and biochemical changes in the nucleus associated with its transition from a highly active state in the basal layer to fully inactive state in the cornified layer, where DNA is degraded and nucleus is eliminated (Botchkarev et al., 2012; Eckhart et al., 2013). Differentiating epidermal keratinocytes markedly change their nuclear shape and three-dimensional (3D) nuclear organization, including spatial relationships between pericentromeric heterochromatin clusters, nucleoli, and chromosome territories (Gdula et al., 2013).

Nuclear shape and size are controlled by the nuclear envelope (NE) that provides anchoring sites for several cytoskeletal components and chromatin at the outer and inner nuclear membranes (NMs), respectively. The NE plays a crucial role in regulating the mechanical stability of the nucleus, nucleocytoplasmic transport, chromatin organization, and gene expression (Hetzer, 2010; Kim et al., 2015; Wilson and Foissner, 2010). Proteins of the linker of nucleoskeleton and cytoskeleton complex (such as nesprins-1/2/3/4) interact directly with the cytoplasmic cytoskeleton on the outer NM. At the inner NM, a different set of linker of nucleoskeleton and cytoskeleton proteins, such as Sun1/2, interact with nuclear lamins, thus forming “bridges” that link outer and inner membranes and establish physical connections between the cytoskeleton and chromatin (Hetzer, 2010; Sosa et al., 2013).

¹Centre for Skin Sciences, University of Bradford, Bradford, UK;

²Department of Dermatology, Boston University School of Medicine, Boston, Massachusetts, USA; and ³Department of Biosciences, University of Durham, Durham, UK

⁴Current address: Centre for Genomics and Child Health, Blizzard Institute, Barts; and the London School of Medicine and Dentistry, Queen Mary University of London, UK.

⁵These authors contributed equally to this work.

Correspondence: Vladimir A. Botchkarev, Centre for Skin Sciences, University of Bradford, Bradford BD7 1DP, UK, E-mail: v.a.botchkarev@bradford.ac.uk; Boston University, 609 Albany Street, Boston, Massachusetts 02118, USA, E-mail: vladbotc@bu.edu; or Andrei Mardaryev, Centre for Skin Sciences, University of Bradford, Bradford BD7 1DP, UK, E-mail: a.mardaryev@bradford.ac.uk

Abbreviations: CC, chromocenter; ChIP-qPCR, chromatin immunoprecipitation-quantitative PCR; H3K9me3, trimethylation on lysine 9 of histone H3; H3K27me3, trimethylation on lysine 27 of histone H3; Kt1, keratin type I; Kt11, keratin type II; PMK, primary mouse keratinocyte; IF, intermediate filament; NM, nuclear membrane; NE, nuclear envelope; WT, wild-type

Received 16 January 2017; revised 20 April 2017; accepted 1 May 2017; accepted manuscript published online 6 June 2017

In keratinocytes, both keratin filaments and nuclear lamins contribute to the regulation of nuclear shape and integrity. Cytokeratin 14 filaments form a cage-like perinuclear structure, which is required for resizing and reshaping of nuclei in early differentiating keratinocytes, whereas *Krt14* gene ablation results in alterations of nuclear shape in epidermal keratinocytes (Lee et al., 2012; Troy and Turksen, 1999). In addition, keratin 1/10 deletion decreases expression of NE-associated proteins, such as emerin, lamin A/C, and Sun1, leading to premature nuclei loss during epidermal differentiation (Wallace et al., 2012).

Nuclear lamins (Lamin A/C, Lamin B1, and Lamin B2) are intermediate filaments (IFs) forming an interconnected meshwork (lamina) underlying the inner NM. They also contribute to the regulation of nuclear shape and link inner NM to the chromatin via interaction with its lamina-associated domains (Hetzer, 2010; Kind et al., 2015). Loss of Lamin A/C and Lamin B receptors leads to the loss of peripheral heterochromatin in many cell types including hair follicle keratinocytes (Solovei et al., 2013). Moreover, genetic ablation of all three nuclear lamins in keratinocytes resulted in the development of ichthyosis and skin barrier defects (Jung et al., 2014).

p63 transcription factor is a master regulator of epidermal development as its deletion leads to profound defects in epidermal morphogenesis (Mills et al., 1999; Yang et al., 1999). p63 controls expression of a large number of genes controlling cell adhesion, signaling, and lineage-specific components of the cytoskeleton, such as keratins (Kouwenhoven et al., 2010, 2015; McDade et al., 2012; Viganò et al., 2006; Zarnegar et al., 2012). We also reported that p63 controls expression of a number of chromatin remodelers, such as Satb1, Brg1, and Cbx4, that coordinate gene expression in epidermal progenitor cells during development (Fessing et al., 2011; Mardaryev et al., 2014, 2016). In this report, we show that p63 regulates the nuclear shape and expression of NE-associated genes, coupled to changes in heterochromatin organization and intranuclear position of keratin loci in keratinocytes. These data suggest a complex role for p63 in the integration of cytoskeleton, NE, and chromatin remodeling factors in epidermal progenitor cell differentiation during morphogenesis.

RESULTS

Skin epithelial cells in p63 knockout mice display nuclear shape alterations

Emerging data suggest that the cytoskeleton plays an important role in nuclear morphology and chromatin organization (Li et al., 2014; Ramdas and Shivashankar, 2015; Xue and Funabiki, 2014). As several p63 targets encode cytoskeletal components, we speculated that p63 may regulate nuclear morphology. To test this, we analyzed expression of NE-associated proteins in E16.5 *p63*^{-/-} embryos and age-matched wild-type (WT) controls. Immunostaining with anti-Lamin B1 and anti-Lamin A/C antibodies revealed an epidermal-specific decrease in expressions of nuclear lamins in *p63*^{-/-} mice compared with controls, whereas dermal cells were not affected (Figure 1a–c; Supplementary Figure S1a and b online). Interestingly, the reduced nuclear

lamin expressions were more profound in cells with abnormal nuclear shape in *p63*^{-/-} keratinocytes (Figure 1a–c, arrowheads). Lamin B1 expression was also reduced in p63-depleted primary mouse keratinocytes (PMKs) transfected with p63-specific siRNA (Figure 1d; Supplementary Figure S2a and b online).

To characterize the nuclear shape changes on p63 deletion, we measured a nuclear circularity index, which defines alterations and variations in the nuclear shape based on how closely each nucleus corresponds to a spherical shape (a perfect sphere has a value of 1). In agreement with previous reports, we considered nuclei with a circularity index <0.8 as altered in shape (Ray and Chapman, 2015; Schochlin et al., 2014). Our analysis revealed that approximately 32% of p63-null keratinocytes had abnormal nuclei with circularity index <0.8 (compared with 0.5% of cells in WT controls) (Figure 1e and g). Furthermore, p63 knockdown in PMKs revealed a significant increase in the number of cells (23%) with altered nuclear shape compared with only 3% of control cells (Figure 1f and h). The nuclear shape changes were keratinocyte specific, as the circularity index was not significantly altered in *p63*^{-/-} dermal cells compared with controls (Supplementary Figure S1b and c).

As changes in the nuclear shape can be caused by apoptosis (Rao et al., 1996; Raz et al., 2006), we analyzed the expression of active caspase-3 in *p63*^{-/-} mice. All epidermal keratinocytes with misshapen nuclei were negative for the caspase-3 (Supplementary Figure S3a online), indicating that alterations in the nuclear shape were associated with mechanisms other than apoptosis in *p63*^{-/-} mice. Consistently with this observation, most cells with misshapen nuclei were actively proliferating as determined by Ki-67 staining (Supplementary Figure S3b).

Decreased expression of NE-associated proteins in p63-null keratinocytes

Because epidermal cells in *p63*^{-/-} mice and p63-depleted PMKs showed a marked reduction in Lamin B1 and Lamin A/C (Figure 1a–d), we asked if other NE-associated proteins were also affected in p63-null epidermis. The analysis of our previously published *p63*^{-/-} transcriptome (Fessing et al., 2011; Mardaryev et al., 2014) revealed a downregulation of 17 transcripts encoding NE and NE-associated proteins in p63-null epidermis compared with controls (Figure 2a).

To validate the microarray data, we selected a list of genes (*Plec*, *Sun1*, *Syne2*, *Syne3*, and *Lmnb1*) for further analysis. We found a significant decrease in expression of the selected genes by quantitative real-time reverse transcriptase–PCR in *p63*^{-/-} keratinocytes versus WT controls (Figure 2b). Immunostaining also confirmed the reduced expression of Plectin, Sun1, and Nesprin-3 proteins in the *p63*^{-/-} epidermis compared with controls (Figure 2c). Furthermore, siRNA-mediated p63 knockdown revealed a significant decrease in expression of *Lmnb1*, *Lmna*, *Plec*, *Sun1*, *Syne2* but not *Syne3* in PMKs (Figure 2d).

p63 binds to the regulatory regions of the *Plec*, *Sun1*, and *Syne3* genes

To test whether the *Sun1*, *Syne3*, *Plec*, and *Lmnb1* genes may be direct p63 targets in keratinocytes, we performed

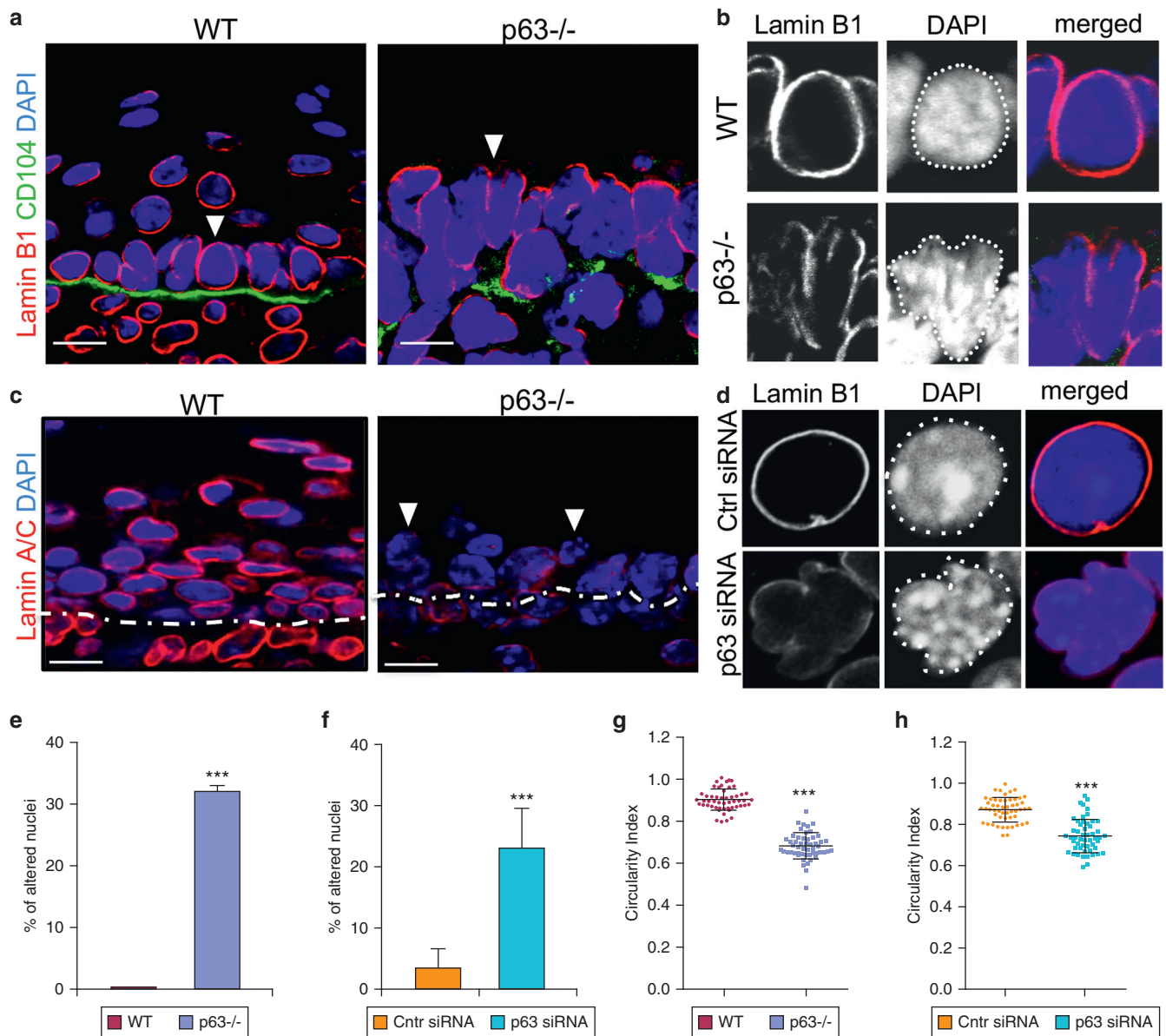


Figure 1. In vivo and in vitro analysis of WT and p63-null keratinocytes nuclear shape. (a, b) In vivo analysis of the nuclear shape of basal keratinocytes in p63-null embryos versus wild-type controls, stained with Lamin B1. CD104 (Integrin b4) staining depicts the basement membrane (a). Arrowheads (a) indicate nuclei shown enlarged (b). Scale bars = 10 μ m. (c) Lamin A/C expression in $p63^{-/-}$ keratinocytes. Note a decreased expression of Lamin A/C in $p63^{-/-}$ keratinocytes with altered nuclear shape (arrowheads). The dashed line delineates the dermal-epidermal junction. Scale bars = 10 μ m. (d) Decreased expression of Lamin B1 and altered nuclear shape in primary mouse keratinocytes transfected with p63 siRNA. (e, f) Quantification of keratinocytes with altered nuclear shape in (e) $p63^{-/-}$ mice and (f) p63-depleted keratinocytes in vitro. Chi-square test (mean \pm SD, *** P -value < 0.001). (g, h) Quantification of the nuclear circularity index in (g) $p63^{-/-}$ mice and (h) p63-depleted keratinocytes in vitro. Student's t -test (mean \pm SD, *** P -value < 0.001). SD, standard deviation; siRNA, small interfering RNA; WT, wild-type.

chromatin immunoprecipitation with anti-p63 antibody followed by quantitative PCR (ChIP-qPCR) analysis in PMKs isolated from newborn WT mice. Using a PatSearch tool (Grillo et al., 2003), we designed qPCR primers to multiple sites within a 6-kb-long region upstream to transcription start sites, containing several putative p63-binding sites (Figure 3a). ChIP-qPCR revealed p63 binding to *Plec*, *Sun1*, and *Syne3* within the analyzed regions (Figure 3b), suggesting that all three genes are direct p63 targets in mice. In contrast, we did not see any p63 enrichment on *Lmnbl1* even by testing multiple predicted sites within the *Lmnbl1* promoter region (Supplementary Figure S4a online),

suggesting an indirect regulation by p63. To test if the same genes targeted by p63 in normal human epidermal keratinocytes, we reanalyzed the publicly available p63 ChIP-seq dataset and ENCODE data for enhancer-specific histone modifications (H3K4me1, H3K27ac) (ENCODE Project Consortium, 2012; Kouwenhoven et al., 2010). Similar to mice, p63 was coenriched with the histone marks in the promoter and proximal enhancer regions (up to 10 kb from transcription start sites) of *PLEC*, *SUN1*, and *SYNE3* in normal human epidermal keratinocytes. However, p63 did not bind to *LMNB1* promoter or distant enhancers even within 50 kb from the transcription start sites (Supplementary Figure S4b).

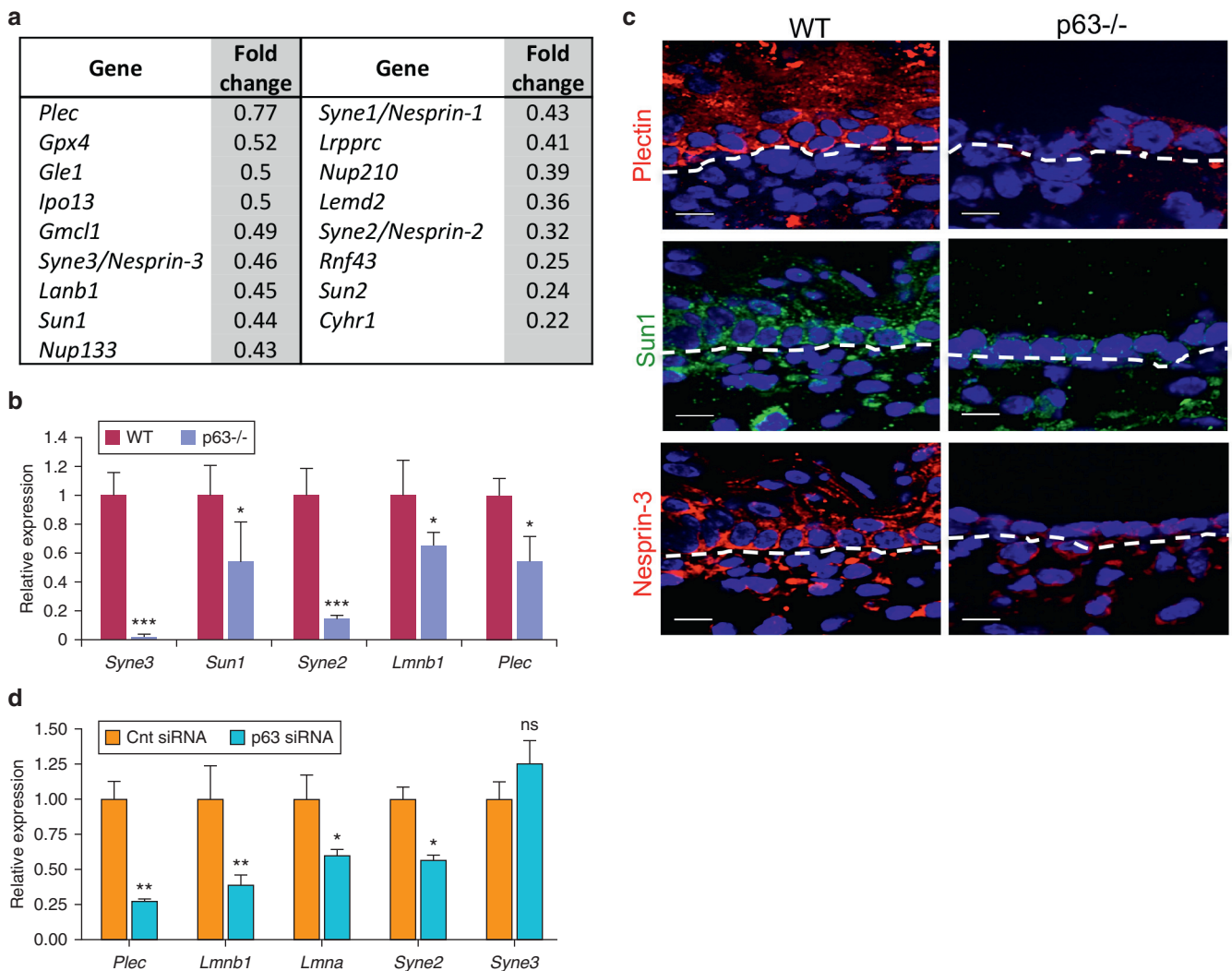


Figure 2. Nuclear envelope-associated proteins are reduced in p63-null keratinocytes. (a) Agilent microarray data demonstrating changes in expression of genes encoding nuclear envelope-associated proteins between *p63*^{-/-} and WT mice. (b) Real-time PCR validation of the microarray analysis for *Plec*, *Sun1*, *Syne3*, *Syne2* and *Lmnb1* in the E16.5 epidermis of *p63*^{-/-} mice normalized to the corresponding levels in the age-matched WT epidermis (mean \pm SD, $n = 3$, * $P < 0.05$, *** $P < 0.001$). (c) Immunostaining for plectin, SUN1 and nesprin-3 in the E16.5 skin of WT and *p63*^{-/-} mice. Scale bar, 10 μ m. Dashed lines depict dermal-epidermal junction. (d) Real-time PCR analysis for *Plec*, *Sun1*, *Syne2/3*, *Lmna* and *Lmnb1* expression in PMK after p63 knockdown using siRNA (mean \pm SD, $n = 3$, * $P < 0.05$, ** $P < 0.001$). PMK, primary mouse keratinocyte; SD, standard deviation; WT, wild-type.

p63-null keratinocytes show an altered heterochromatin organization

Reduced levels of lamins and other NE proteins alter the distribution of trimethylation on lysine 27 of histone H3 (H3K27me3) and trimethylation on lysine 9 of histone H3 (H3K9me3) histone modifications, established markers of transcriptionally inactive chromatin (Kim and Kim, 2012; Le et al., 2016; Shumaker et al., 2006). Our analysis revealed a global decrease of H3K27me3 in p63-null keratinocytes compared with controls (Figure 4a and b). Although H3K27me3 was significantly enriched at the nuclear periphery in close contacts with the nuclear lamina in WT keratinocytes, it was evenly distributed within the nuclei in p63-null keratinocytes (Figure 4c; Supplementary Figure S5a online). Because polycomb repressive complex 2 is responsible for H3K27me3 deposition in keratinocytes (Bardot et al., 2013; Ezhkova et al., 2009, 2011; Perdigoto et al., 2016), we analyzed expression of its subunits in

p63-null mice. Although there were no changes in *Ezh1* and *Eed* expression, *Ezh2* and *Suz12* were significantly reduced in the epithelium of *p63*^{-/-} mice compared with WT controls (Figure 4d–f; Supplementary Figure S6a online). Furthermore, a polycomb repressive complex 1-dependent histone modification (H2AK119Ub) was reduced in the p63-null epidermis but not in the dermal cells (Supplementary Figure S6b–d). As *Ring1* and *Rnf2/Ring1b*, catalytic subunits of polycomb repressive complex 1, were not decreased in the p63-null cells (Supplementary Figure S6e and f), the H2AK119Ub1 reduction was likely caused by the decreased polycomb repressive complex 2 activity in p63-null cells (Schwartz and Pirrotta, 2013; van Kruijsbergen et al., 2015).

Analysis of H3K9me3, a histone modification associated with the pericentromeric heterochromatin, revealed its altered distribution with a significant increase of H3K9me3 foci at the nuclear interior in p63-null keratinocytes compared with controls (Figure 4g and h). Quantification of H3K9me3 foci showed that

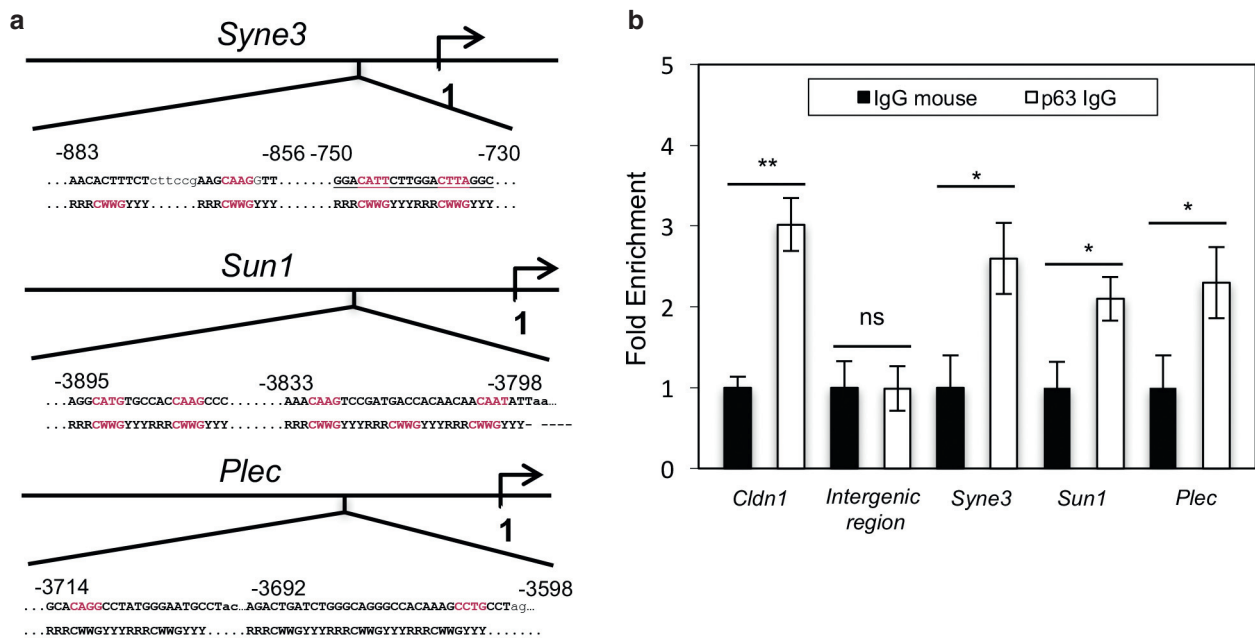


Figure 3. p63 is enriched at the promoter regions of the *Syne3*, *Sun1*, and *Plec* genes. Chromatin isolated from primary mouse keratinocytes was processed for ChIP assay with an antibody against p63 protein or purified mouse IgG. (a) Regions within the promoter of *Syne3*, *Sun1*, and *Plec* analyzed by ChIP-qPCR. Matching p63 core binding site consensus sequences are in red. (b) Enrichment of p63 at the *Syne3*, *Sun1*, and *Plec* promoter regions. The input levels of unprecipitated chromatin DNA were used as loading controls. *Cldn1* and an intergenic region on chr. 8 were used as positive and negative controls, respectively. Error bars represent SD, and four independent experiments were run in triplicates; $P < 0.05$. ChIP-qPCR, chromatin immunoprecipitation-quantitative PCR; SD, standard deviation.

they were more numerous (approximately 12 foci/nucleus) and smaller in size in p63-null nuclei compared with the controls (approximately 8 foci/nucleus) (Figure 4g; Supplementary Figure S5b online), suggesting that heterochromatin clustering and organization was affected in p63-deficient cells. In line with these observations, we found a reduced expression of HP1 α , which interacts with H3K9me3 and is responsible for the pericentromeric heterochromatin organization and clustering (Jones et al., 2000), as well as the loss of its peripheral localization in p63-null nuclei compared with WT controls (Figure 4i and j).

Furthermore, we found a greater reduction and loss of H3K27me3 and H3K9me3 peripheral distribution in cells with abnormal nuclei compared with cells with relatively normal nuclear shape in p63 $^{-/-}$ mice (Supplementary Figure S5c and d online). The latter suggests that there is a direct correlation between nuclear shape alterations and changes in heterochromatin reorganization in p63 $^{-/-}$ mice.

Keratinocyte-specific gene loci relocate away from the sites of active transcription toward constitutive heterochromatin in p63 $^{-/-}$ mice

Keratin genes are profoundly downregulated in p63 $^{-/-}$ mice (Supplementary Figure S7 online) and clustered in two distinct genomic loci, keratin type I (KtyI) and keratin type II (KtyII), located on mouse chromosomes 11 and 15, respectively (Fessing et al., 2011; Koster et al., 2006; Truong et al., 2006; Viganò et al., 2006).

To test whether the alterations in heterochromatin organization affect intranuclear positioning of keratin genes and contribute to their transcriptional silencing in p63 $^{-/-}$ mice, we performed 3D fluorescence in situ hybridization experiments on WT and

p63 $^{-/-}$ mouse skin at E16.5 using DNA probes covering KtyI and KtyII loci. The FISH probes were coimmunostained with an antibody against the elongating form of RNA polymerase II phosphorylated at Ser-2, which is enriched in actively transcribed genomic regions (Estarras et al., 2013; Srivastava and Ahn, 2015; Zentner et al., 2011). Both KtyI and KtyII loci were localized in the nuclear interior enriched in RNA polymerase II phosphorylated at Ser-2 in WT cells (Figure 5a and b). In striking contrast, KtyI and KtyII loci in p63-null keratinocytes were found predominantly in RNA polymerase II phosphorylated at Ser-2-depleted sites in close proximity to DAPI-dense chromocenters (CCs), the sites of pericentromeric heterochromatin (Figure 5a and b). Quantification of the KtyI/II loci association with CCs revealed a striking increase in the number of cells where both alleles of keratin loci were in close contact with CCs in p63 $^{-/-}$ keratinocytes compared with WT cells (Figure 5c and d). In contrast, the number of nuclei where no such contacts observed was dramatically reduced in p63-null keratinocytes compared with controls (Figure 5c–e).

The observed data are intriguing, as CCs are known to be the clusters of pericentromeric satellite repeats of chromosomes that cosegregate and comprise the constitutive heterochromatin creating a repressive environment in the nucleus (Politz et al., 2013; Wijchers et al., 2015). Furthermore, CCs are enriched in heterochromatin marks, such as H3K9me2/3 (Supplementary Figure S5e online) (Lienert et al., 2011; Magklara et al., 2011). Together, these data demonstrate that KtyI/II loci relocate to a repressive environment composed of constitutive heterochromatin in p63-null keratinocytes, which highlights a causative link between nuclear shape alterations and heterochromatin redistribution that

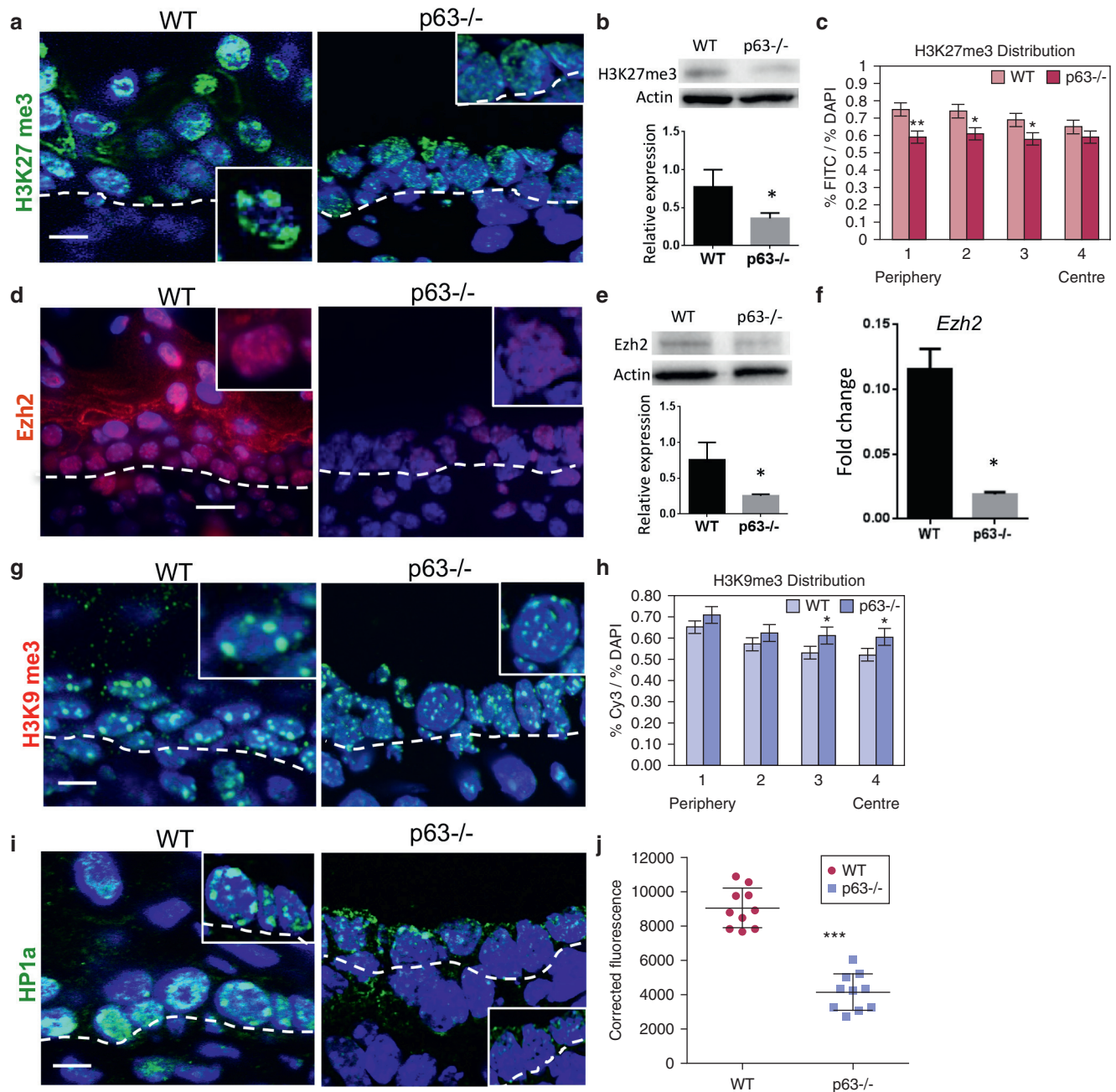


Figure 4. Alterations in the nuclear distribution of heterochromatin in *p63*^{-/-} epidermis. Immunofluorescence analysis for H3K27me3, Ezh2, H3K9me3, HP1a in the E16.5 skin of WT and *p63*^{-/-} mice. Dashed lines depict the dermal-epidermal junction. **(a, b)** Reduced expression of H3K27me3 in *p63*-null keratinocytes detected by **(a)** immunofluorescent and **(b)** western blot analyses ($n = 2$, mean \pm SD, $*P < 0.05$). Scale bar = 10 μ m. **(c)** Loss of H3K27me3 peripheral distribution in *p63*-null (one-way ANOVA test, mean \pm SEM, $*P < 0.05$, $**P < 0.01$). **(d–f)** Significant decrease of **(d, e)** Ezh2 protein and **(f)** transcript expression in *p63*-null epidermis ($n = 2$, mean \pm SD, $*P = 0.05$). Scale bar = 10 μ m. **(g, h)** Altered distribution pattern of H3K9me3 with a significant increase of its internal distribution ($*P = 0.03$) in *p63*-null keratinocytes (mean \pm SEM, $n = 3$). Scale bar = 10 μ m. **(i, j)** Marked decrease of HP1a in *p63*-null epidermis compared with wild-type control ($***P < 0.001$, mean \pm SD, $n = 3$). Scale bar = 10 μ m. ANOVA, analysis of variance; SD, standard deviation; SEM, standard error of the mean; WT, wild-type.

lead to changes in intranuclear gene positioning and expression of keratinocyte-specific genes in *p63*^{-/-} mice.

DISCUSSION

Here, we show that p63 regulates nuclear shape in epidermal progenitor cells during skin development. Both in vivo and in vitro studies revealed a significant portion of *p63*-deficient keratinocytes with misshapen nuclei associated with

a marked decrease in nuclear lamins and NE-associated proteins. Previous studies showed that murine cells lacking nuclear lamins or cells from patients with Hutchinson-Gilford progeria syndrome, harboring Lamin A mutations, display misshapen nuclei similar to those observed in *p63*-null keratinocytes (Goldman et al., 2004; Jung et al., 2014; Lammerding et al., 2004; Vergnes et al., 2004; Yang et al., 2011). Together, these observations suggest that reduced

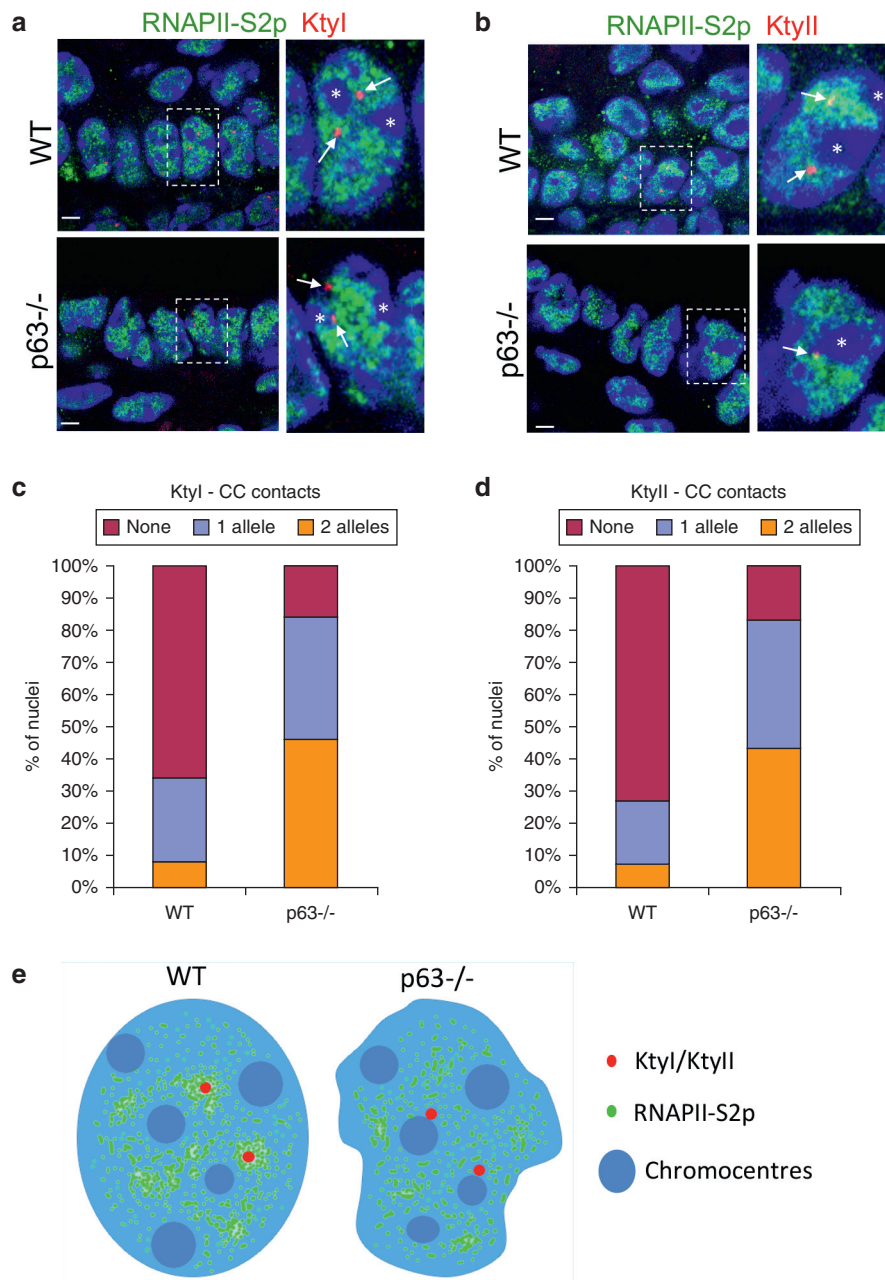


Figure 5. Relocation of keratinocyte-specific gene loci toward chromocenters in *p63*^{-/-} epidermis.

(a, b) Multicolor 3D-FISH with probes for (a, arrows) Ktyl or (b, arrows) KtyII followed by immunodetection of pSer2-Pol II in the epidermis of *p63*^{-/-} and control mice at E16.5; * labels chromocenters. Scale bars = 5 μ m. (c, d) *p63*-null keratinocytes show an increase in the portion of nuclei where both alleles of (c) Ktyl or (d) KtyII are closely associated with the chromocenters (CCs) ($n = 50$). (e) A schematic diagram depicting the position of Ktyl and KtyII loci relative to DAPI-dense chromocenters and polymerase II-enriched active site of transcription. 3D-FISH, 3D fluorescence in situ hybridization; Ktyl, keratin type I; KtyII, keratin type II; WT, wild-type.

expression of Lamin B1 and Lamin A/C may contribute to the defects in nuclear shape observed in *p63*^{-/-} mice. However, *Lmnb1* and *Lmna* are likely regulated indirectly by p63, as we could not identify enrichment of p63 at the promoter regions of both genes. Nevertheless, the nuclear lamin reduction may significantly contribute to the skin defects in *p63*^{-/-} mice, as the triple lamin knockout mice develop defective epidermal barrier and hypotrophic hair follicles (Jung et al., 2014).

In addition to nuclear lamins, several NE-associated proteins, including plectin, nesprin-3, and Sun1, were significantly downregulated in *p63*-null keratinocytes. Plectin is a cytoskeletal linker protein of the plakin family that is associated with filamentous actin, IFs, and hemidesmosomal integrins in basal keratinocytes (Nievers et al., 2000;

Reznicek et al., 1998). Plectin is also required for attachment of the nucleus to cytoplasmic IFs via interaction with the linker of nucleoskeleton and cytoskeleton protein nesprin-3 (Ketema et al., 2013; Wilhelmsen et al., 2005). Loss of plectin in keratinocytes reduces keratin IF density around the nucleus and leads to abnormal nuclear morphology. The latter is linked to several skin defects, associated with extremely fragile epidermis and severe skin lesions, including the epidermolysis bullosa complex (Ackert et al., 2007; Almeida et al., 2015; Gostynska et al., 2015).

Nesprin-3 can uniquely link the NE to the IF network and is also suggested to be involved in maintaining the structural integrity and shape of the nucleus (reviewed in Ketema and Sonnenberg, 2011). Nesprin-3 maintains perinuclear cytoskeleton architecture in endothelial cells and *Zebrafish*

epidermal cells (Morgan et al., 2011; Postel et al., 2011). However, the role of nesprin-3 in the homeostasis of mammalian epidermis remains unclear. Loss of nesprin-2 (structurally related to nesprin-3) in human keratinocytes results in variable NE morphological changes from minor NE blebbing to severely misshapen and giant nuclei (Luke et al., 2008). The largest isoforms of *Syne1* and *Syne2* loci termed nesprin-1 and nesprin-2 giant, respectively, interact directly with nesprin-3 via their N-terminal actin binding domains at the outer NM. Collectively, this suggests that nesprin-3 may also regulate the nuclear shape in keratinocytes either via plectin-mediated binding to IFs or by modulating the nesprin-1 and -2 interplay with the cytoskeleton (Lu et al., 2012).

As a part of the linker of nucleoskeleton and cytoskeleton complex, Sun1 is important for localization of nesprins at the outer NM and their interaction with the nuclear lamina (Padmakumar et al., 2005). Sun1-null mice show defects in the formation and positioning of nuclei and cellular dysfunction in several tissues (Ding et al., 2007; Horn et al., 2013; Lei et al., 2009). Sun proteins also play a critical role in the maintenance of epidermal integrity. Downregulations of Sun1 expression along with lamin A/C and emerin were detected in K1/K10-null mice leading to premature nuclear loss during epidermal differentiation (Wallace et al., 2012). Deletion of Sun2, a functional homologue of Sun1, also showed aberrant nuclear position, altered desmosome distribution, and mechanically defective adhesions resulting in defective hair follicle structure and alopecia (Stewart et al., 2015).

Collectively, our data suggest that downregulation of nuclear lamins and NE-associated proteins can lead to the nuclear shape alterations observed in p63-null keratinocytes. To date, it is unclear whether the maintenance of correct nuclear shape by p63 influences p63-dependent gene expression program during epidermal development. Our data provide some answer to the question by revealing that p63 is involved in the control of heterochromatin organization, which is frequently associated with the nuclear periphery in close contacts with nuclear lamins and lamina-associated components (Bank and Gruenbaum, 2011). We showed that p63 deletion in keratinocytes reduces Ezh2 and HP1a expressions and alters the distribution of heterochromatin-associated H3K27me3, H2AK119ub1, and H3K9me3 histone marks suggesting that heterochromatin organization is affected in these cells. In line with these observations, Ktyl and Ktyll gene loci move away from the RNA polymerase II phosphorylated at Ser-2-enriched sites of active transcription toward the heterochromatin-enriched CCs in p63-null keratinocytes. Collectively, these data raise an intriguing possibility that p63 maintains an active transcriptional environment around the highly expressed keratin genes and prevents heterochromatin redistribution and/or spreading, at least in part, via regulating the expression of NE-associated proteins and controlling a proper nuclear shape. Our finding is also supported by a recent observation that mechanical force-dependent depletion of NE-associated protein emerin alters the H3K9me2/3 and H3K27me3 levels leading to chromatin rearrangements and reduced transcription of lineage-specific genes in human epidermal progenitor cells (Le et al., 2016).

Other p63-dependent mechanisms can also be involved in maintaining the high transcriptional state in keratin loci in epithelial cells. We previously showed that p63 directly regulates the expression of ATP-dependent chromatin remodeler Brg1, which contributes to a developmentally regulated relocation of the epidermal differentiation complex locus toward the transcriptionally active nuclear interior in epidermal progenitor cells (Mardaryev et al., 2014). A similar function for Brg1 was demonstrated in other cell lineages (Christova et al., 2007; Clapier and Cairns, 2009). However, the role of Brg1 in the control of Ktyl/II loci nuclear positioning in keratinocytes requires further investigations.

In summary, our data demonstrate a previously unreported role of p63 in coupling the cytoskeleton and nuclear shape regulation with a 3D nuclear organization as an essential part of p63-dependent gene expression program. By regulating expression of NE-associated genes, p63 is involved in maintaining facultative and constitutive heterochromatin organization in epidermal keratinocytes. However, more detailed and genome-wide studies are required to address to what degree the nuclear shape regulation and heterochromatin organization contribute to the p63-dependent gene expression program keratinocytes. In particular, DNA adenine methyltransferase identification analysis in p63-null keratinocytes will be important to identify changes in the lamina-associated domains that dynamically associate with lamina and contain many developmentally regulated and/or tissue-specific genes (Lin et al., 2012; Meister et al., 2010; Peric-Hupkes et al., 2010). Future research in this direction will shed some more light on the complex p63-dependent regulatory network that controls epidermal development and its maintenance, as well as provides a mechanistic insight into the pathological conditions with underlined p63 dysfunction.

MATERIALS AND METHODS

Experimental animals and tissue collection

Animal studies were performed in accordance with protocols approved by the UK Home Office Project License. C57Bl/6 mice were purchased from Charles River. p63-null and WT embryos were obtained by breeding p63^{+/-} animals from Jackson Laboratories. Skin samples were collected from mice at distinct days of embryonic and postnatal development (E16.5 and P0.5), as described previously (Botchkarev et al., 1999b; Sharov et al., 2003, 2005). Genotyping of mice was performed using PCR, as recommended by the supplier. For each developmental stage, six to seven samples were collected. Tissue samples were covered in Tissue-Tek O.C.T. Compound (VWR, Lutterworth, UK), snap-frozen in liquid nitrogen, and stored in -80 °C.

Immunofluorescence, 3D fluorescence in situ hybridization, and image analysis

Histological sections of quick frozen E16.5 p63^{-/-} and age-matched WT embryos were fixed in 4% paraformaldehyde and stained with specific primary and secondary antibodies (Supplementary Table S1 online), as described previously (Botchkarev et al., 1999a; Fessing et al., 2006; Sharov et al., 2003, 2005). Nuclei of basal keratinocytes from p63^{-/-} mice, p63 siRNA-treated PMKs, and corresponding control cells were counted using ImageJ software and percentages of nuclei with altered morphology were calculated in Microsoft Excel spreadsheets. Circularity values were obtained using

“Circularity” ImageJ plugin (<http://rsb.info.nih.gov/ij/plugins/circularity.html>).

For the analysis of the distribution of histone modifications, the nuclear geometric center of nuclei ($n = 35$) from both WT and $p63^{-/-}$ embryos was found and lines were drawn from the nuclear center to the nuclear periphery. To cover the entire nuclear surface, eight radial lines have been drawn throughout the nuclear center and values of fluorescence intensity have been collected using ImageJ plugin “Plot Profile.” Measurements from each line have been subsequently divided and grouped into four different shells, averaged and normalized to the mean percentage of DAPI signal in that shell.

Immunofluorescence intensity was determined using ImageJ software, as described previously (Mardaryev et al., 2016). Briefly, regions of interest were selected within WT or $p63^{-/-}$ epidermis and dermis, and the corrected values of total cell fluorescence (CTCF) were calculated for each selected areas using the following formula: $CTCF = \text{Integrated Density} - (\text{Area of selected cell} \times \text{Mean fluorescence of background readings})$. For pairwise comparisons, a two-tailed t -test ($\alpha = 0.05$) was employed.

DNA probe preparation and 3D fluorescence in situ hybridization analysis were performed as described previously (Fessing et al., 2011; Mardaryev et al., 2014). 3D images were collected using a Zeiss LSM510 confocal microscope. Images were processed and analyzed using ImageJ. DAPI-enriched CCs were considered to be within the vicinity of gene loci when the corresponding fluorescent signals were found to at least partially overlap.

Laser capture microdissection and quantitative real-time reverse transcriptase-PCR analysis

Laser capture microdissection of whole mouse epidermis of E16.5 $p63^{-/-}$ and age-matched WT controls was performed followed by RNA extraction and amplification, as published before (Fessing et al., 2011). Total RNA was extracted using the ReliaPrep RNA Cell Miniprep System kit (Promega, Southampton, UK), followed by two rounds of amplification using the RiboAmp RNA amplification kit (Life Technologies, Waltham, MA). For quantitative real-time reverse transcriptase-PCR analysis, RNA was retrotranscribed into cDNA and specific primers were designed using the Beacon Designer software (Supplementary Table S2 online; PREMIER Biosoft International, Palo Alto, CA). Real-time PCR was performed using SYBER-Green Master Mix (Life Technologies) on the StepOne Plus system (Life Technologies). Differences between samples were calculated based on the C_t ($\Delta\Delta C_t$) method and normalized to *Gapdh*. Data from triplicates were pooled, mean \pm standard deviation was calculated, and statistical analysis was performed using unpaired Student's t -test.

Cell culture and siRNA transfection

PMKs were isolated from newborn 2- to 3-day-old C57BL/6 mice, as described previously (Lewis et al., 2014; Mardaryev et al., 2016). PMKs were grown in EMEM calcium-free medium (Lonza, Waltham, UK) with supplements (0.05 mM calcium, 4% fetal bovine serum, 0.4 $\mu\text{g/ml}$ hydrocortisone, 5 $\mu\text{g/ml}$ insulin, 10 mg/ml epidermal growth factor (EGF), 10^{-10} M cholera toxin, 2×10^{-9} T3, 2 mM L-glutamine, 100 U/ml penicillin, and 100 $\mu\text{g/ml}$ streptomycin) at 33 °C, 8% CO_2 until 60–70% confluent. PMKs were transfected with 100 nM p63siRNA or control siRNA using Lipofectamin 2000 (Life Technologies).

ChIP-qPCR assay

ChIP assay was performed using epidermal keratinocytes isolated from newborn mouse skin with a p63 antibody or IgG control, as published

previously (Mardaryev et al., 2011). Briefly, cross-linked DNA after sonication was precipitated with 5 μg of anti-p63 antibody or nonimmune goat IgG (Vector Laboratories, Burlingame, CA) overnight at 4 °C. Purified ChIPed DNA was amplified with gene specific primers (Supplementary Table S3 online). ChIP-qPCR data from triplicates were pooled, mean \pm standard deviation was calculated, and statistical analysis was performed using Student's t -test.

CONFLICT OF INTEREST

The authors state no conflict of interest.

ACKNOWLEDGMENTS

This work was supported by the grants from Biotechnology and Biological Sciences Research Council (BB/K010050/1), Medical Research Council (MR/M010015/1), and National Institute of Arthritis and Musculoskeletal and Skin Diseases (AR064580) to VAB, as well as by the grant from MRC (MR/N009630/1) to AM.

SUPPLEMENTARY MATERIAL

Supplementary material is linked to the online version of the paper at www.jidonline.org, and at <http://dx.doi.org/10.1016/j.jid.2017.05.013>.

REFERENCES

- Ackerl R, Walko G, Fuchs P, Fischer I, Schmuth M, Wiche G. Conditional targeting of plectin in prenatal and adult mouse stratified epithelia causes keratinocyte fragility and lesional epidermal barrier defects. *J Cell Sci* 2007;120(Pt 14):2435–43.
- Almeida FV, Walko G, McMillan JR, McGrath JA, Wiche G, Barber AH, et al. The cytolinker plectin regulates nuclear mechanotransduction in keratinocytes. *J Cell Sci* 2015;128:4475–86.
- Bank EM, Gruenbaum Y. The nuclear lamina and heterochromatin: a complex relationship. *Biochem Soc Trans* 2011;39:1705–9.
- Bardot ES, Valdes VJ, Zhang J, Perdigoto CN, Nicolis S, Hearn SA, et al. Polycomb subunits Ezh1 and Ezh2 regulate the Merkel cell differentiation program in skin stem cells. *EMBO J* 2013;32:1990–2000.
- Blanpain C, Fuchs E. Epidermal homeostasis: a balancing act of stem cells in the skin. *Nat Rev Mol Cell Biol* 2009;10:207–17.
- Botchkarev VA, Botchkareva NV, Roth W, Nakamura M, Chen LH, Herzog W, et al. Noggin is a mesenchymally derived stimulator of hair-follicle induction. *Nat Cell Biol* 1999a;1:158–64.
- Botchkarev VA, Gdula MR, Mardaryev AN, Sharov AA, Fessing MY. Epigenetic regulation of gene expression in keratinocytes. *J Invest Dermatol* 2012;132:2505–21.
- Botchkarev VA, Peters EM, Botchkareva NV, Maurer M, Paus R. Hair cycle-dependent changes in adrenergic skin innervation, and hair growth modulation by adrenergic drugs. *J Invest Dermatol* 1999b;113:878–87.
- Christova R, Jones T, Wu PJ, Bolzer A, Costa-Pereira AP, Watling D, et al. P-STAT1 mediates higher-order chromatin remodelling of the human MHC in response to IFN γ . *J Cell Sci* 2007;120(Pt 18):3262–70.
- Clapier CR, Cairns BR. The biology of chromatin remodeling complexes. *Annu Rev Biochem* 2009;78:273–304.
- Ding X, Xu R, Yu J, Xu T, Zhuang Y, Han M. SUN1 is required for telomere attachment to nuclear envelope and gametogenesis in mice. *Dev Cell* 2007;12:863–72.
- Eckhart L, Lippens S, Tschachler E, Declercq W. Cell death by cornification. *Biochim Biophys Acta* 2013;1833:3471–80.
- ENCODE Project Consortium. An integrated encyclopedia of DNA elements in the human genome. *Nature* 2012;489:57–74.
- Estaras C, Fueyo R, Akizu N, Beltran S, Martinez-Balbas MA. RNA polymerase II progression through H3K27me3-enriched gene bodies requires JMJD3 histone demethylase. *Mol Biol Cell* 2013;24:351–60.
- Ezhkova E, Lien WH, Stokes N, Pasolli HA, Silva JM, Fuchs E. EZH1 and EZH2 govern histone H3K27 trimethylation and are essential for hair follicle homeostasis and wound repair. *Genes Dev* 2011;25:485–98.
- Ezhkova E, Pasolli HA, Parker JS, Stokes N, Su IH, Hannon G, et al. Ezh2 orchestrates gene expression for the stepwise differentiation of tissue-specific stem cells. *Cell* 2009;136:1122–35.

- Fessing MY, Mardaryev AN, Gdula MR, Sharov AA, Sharova TY, Rapisarda V, et al. p63 regulates Satb1 to control tissue-specific chromatin remodeling during development of the epidermis. *J Cell Biol* 2011;194:825–39.
- Fessing MY, Sharova TY, Sharov AA, Atoyan R, Botchkarev VA. Involvement of the Edar signaling in the control of hair follicle involution (catagen). *Am J Pathol* 2006;169:2075–84.
- Fuchs E. Scratching the surface of skin development. *Nature* 2007;445:834–42.
- Gdula MR, Poterlowicz K, Mardaryev AN, Sharov AA, Peng Y, Fessing MY, et al. Remodeling of three-dimensional organization of the nucleus during terminal keratinocyte differentiation in the epidermis. *J Invest Dermatol* 2013;133:2191–201.
- Goldman RD, Shumaker DK, Erdos MR, Eriksson M, Goldman AE, Gordon LB, et al. Accumulation of mutant lamin A causes progressive changes in nuclear architecture in Hutchinson-Gilford progeria syndrome. *Proc Natl Acad Sci USA* 2004;101:8963–8.
- Gostynska KB, Nijenhuis M, Lemmink H, Pas HH, Pasmooij AM, Lang KK, et al. Mutation in exon 1a of PLEC, leading to disruption of plectin isoform 1a, causes autosomal-recessive skin-only epidermolysis bullosa simplex. *Hum Mol Genet* 2015;24:3155–62.
- Grillo G, Licciulli F, Liuni S, Sbisà E, Pesole G. PatSearch: a program for the detection of patterns and structural motifs in nucleotide sequences. *Nucleic Acids Res* 2003;31:3608–12.
- Hetzler MW. The nuclear envelope. *Cold Spring Harb Perspect Biol* 2010;2:a000539.
- Horn HF, Brownstein Z, Lenz DR, Shivatzki S, Dror AA, Dagan-Rosenfeld O, et al. The LINC complex is essential for hearing. *J Clin Invest* 2013;123:740–50.
- Jones DO, Cowell IG, Singh PB. Mammalian chromodomain proteins: their role in genome organisation and expression. *Bioessays* 2000;22:124–37.
- Jung HJ, Tatar A, Tu Y, Nobumori C, Yang SH, Goulbourne CN, et al. An absence of nuclear lamins in keratinocytes leads to ichthyosis, defective epidermal barrier function, and intrusion of nuclear membranes and endoplasmic reticulum into the nuclear chromatin. *Mol Cell Biol* 2014;34:4534–44.
- Ketema M, Kreft M, Secades P, Janssen H, Sonnenberg A. Nesprin-3 connects plectin and vimentin to the nuclear envelope of Sertoli cells but is not required for Sertoli cell function in spermatogenesis. *Mol Biol Cell* 2013;24:2454–66.
- Ketema M, Sonnenberg A. Nesprin-3: a versatile connector between the nucleus and the cytoskeleton. *Biochem Soc Trans* 2011;39:1719–24.
- Kim DH, Li B, Si F, Phillip JM, Wirtz D, Sun SX. Volume regulation and shape bifurcation in the cell nucleus. *J Cell Sci* 2015;128:3375–85.
- Kim J, Kim H. Recruitment and biological consequences of histone modification of H3K27me3 and H3K9me3. *ILAR J* 2012;53:232–9.
- Kind J, Pagie L, de Vries SS, Nahidiazar L, Dey SS, Bienko M, et al. Genome-wide maps of nuclear lamina interactions in single human cells. *Cell* 2015;163:134–47.
- Koster MI, Kim S, Huang J, Williams T, Roop DR. TAP63alpha induces AP-2gamma as an early event in epidermal morphogenesis. *Dev Biol* 2006;289:253–61.
- Kouwenhoven EN, Oti M, Niehues H, van Heeringen SJ, Schalkwijk J, Stunnenberg HG, et al. Transcription factor p63 bookmarks and regulates dynamic enhancers during epidermal differentiation. *EMBO Rep* 2015;16:863–78.
- Kouwenhoven EN, van Heeringen SJ, Tena JJ, Oti M, Dutilh BE, Alonso ME, et al. Genome-wide profiling of p63 DNA-binding sites identifies an element that regulates gene expression during limb development in the 7q21 SHFM1 locus. *PLoS Genet* 2010;6:e1001065.
- Lammerding J, Schulze PC, Takahashi T, Kozlov S, Sullivan T, Kamm RD, et al. Lamin A/C deficiency causes defective nuclear mechanics and mechanotransduction. *J Clin Invest* 2004;113:370–8.
- Le HQ, Ghatak S, Yeung CY, Tellkamp F, Gunschmann C, Dieterich C, et al. Mechanical regulation of transcription controls Polycomb-mediated gene silencing during lineage commitment. *Nat Cell Biol* 2016;18:864–75.
- Lee CH, Kim MS, Chung BM, Leahy DJ, Coulombe PA. Structural basis for heteromeric assembly and perinuclear organization of keratin filaments. *Nat Struct Mol Biol* 2012;19:707–15.
- Lei K, Zhang X, Ding X, Guo X, Chen M, Zhu B, et al. SUN1 and SUN2 play critical but partially redundant roles in anchoring nuclei in skeletal muscle cells in mice. *Proc Natl Acad Sci USA* 2009;106:10207–12.
- Lewis CJ, Mardaryev AN, Poterlowicz K, Sharova TY, Aziz A, Sharpe DT, et al. Bone morphogenetic protein signaling suppresses wound-induced skin repair by inhibiting keratinocyte proliferation and migration. *J Invest Dermatol* 2014;134:827–37.
- Li Q, Kumar A, Makhija E, Shivashankar GV. The regulation of dynamic mechanical coupling between actin cytoskeleton and nucleus by matrix geometry. *Biomaterials* 2014;35:961–9.
- Lienert F, Mohn F, Tiwari VK, Baubec T, Roloff TC, Gaidatzis D, et al. Genomic prevalence of heterochromatic H3K9me2 and transcription do not discriminate pluripotent from terminally differentiated cells. *PLoS Genet* 2011;7:e1002090.
- Lin YC, Benner C, Mansson R, Heinz S, Miyazaki K, Miyazaki M, et al. Global changes in the nuclear positioning of genes and intra- and interdomain genomic interactions that orchestrate B cell fate. *Nat Immunol* 2012;13:1196–204.
- Lu W, Schneider M, Neumann S, Jaeger VM, Taranum S, Munck M, et al. Nesprin interchain associations control nuclear size. *Cell Mol Life Sci* 2012;69:3493–509.
- Luke Y, Zaim H, Karakesisoglou I, Jaeger VM, Sellin L, Lu W, et al. Nesprin-2 Giant (NUANCE) maintains nuclear envelope architecture and composition in skin. *J Cell Sci* 2008;121(Pt 11):1887–98.
- Magklara A, Yen A, Colquitt BM, Clowney EJ, Allen W, Markenscoff-Papadimitriou E, et al. An epigenetic signature for monoallelic olfactory receptor expression. *Cell* 2011;145:555–70.
- Mardaryev AN, Gdula MR, Yarker JL, Emelianov VU, Poterlowicz K, Sharov AA, et al. p63 and Brg1 control developmentally regulated higher-order chromatin remodelling at the epidermal differentiation complex locus in epidermal progenitor cells. *Development* 2014;141:101–11.
- Mardaryev AN, Liu B, Rapisarda V, Poterlowicz K, Malashchuk I, Rudolf J, et al. Cbx4 maintains the epithelial lineage identity and cell proliferation in the developing stratified epithelium. *J Cell Biol* 2016;212:77–89.
- Mardaryev AN, Meier N, Poterlowicz K, Sharov AA, Sharova TY, Ahmed MI, et al. Lhx2 differentially regulates Sox9, Tcf4 and Lgr5 in hair follicle stem cells to promote epidermal regeneration after injury. *Development* 2011;138:4843–52.
- McDade SS, Henry AE, Pivato GP, Kozarewa I, Mitsopoulos C, Fenwick K, et al. Genome-wide analysis of p63 binding sites identifies AP-2 factors as co-regulators of epidermal differentiation. *Nucleic Acids Res* 2012;40:7190–206.
- Meister P, Towbin BD, Pike BL, Ponti A, Gasser SM. The spatial dynamics of tissue-specific promoters during C. elegans development. *Genes Dev* 2010;24:766–82.
- Mills AA, Zheng B, Wang XJ, Vogel H, Roop DR, Bradley A. p63 is a p53 homologue required for limb and epidermal morphogenesis. *Nature* 1999;398:708–13.
- Morgan JT, Pfeiffer ER, Thirkill TL, Kumar P, Peng G, Fridolfsson HN, et al. Nesprin-3 regulates endothelial cell morphology, perinuclear cytoskeletal architecture, and flow-induced polarization. *Mol Biol Cell* 2011;22:4324–34.
- Nievers MG, Kuikman I, Geerts D, Leigh IM, Sonnenberg A. Formation of hemidesmosome-like structures in the absence of ligand binding by the (alpha)6(beta)4 integrin requires binding of HD1/plectin to the cytoplasmic domain of the (beta)4 integrin subunit. *J Cell Sci* 2000;113(Pt 6):963–73.
- Padmakumar VC, Libotte T, Lu W, Zaim H, Abraham S, Noegel AA, et al. The inner nuclear membrane protein Sun1 mediates the anchorage of Nesprin-2 to the nuclear envelope. *J Cell Sci* 2005;118(Pt 15):3419–30.
- Perdigoto CN, Dauber KL, Bar C, Tsai PC, Valdes VJ, Cohen I, et al. Polycomb-mediated repression and sonic hedgehog signaling interact to regulate merkel cell specification during skin development. *PLoS Genet* 2016;12:e1006151.
- Peric-Hupkes D, Meuleman W, Pagie L, Bruggeman SW, Solovei I, Brugman W, et al. Molecular maps of the reorganization of genome-nuclear lamina interactions during differentiation. *Mol Cell* 2010;38:603–13.
- Politz JC, Scalzo D, Groudine M. Something silent this way forms: the functional organization of the repressive nuclear compartment. *Annu Rev Cell Dev Biol* 2013;29:241–70.
- Postel R, Ketema M, Kuikman I, de Pereda JM, Sonnenberg A. Nesprin-3 augments peripheral nuclear localization of intermediate filaments in zebrafish. *J Cell Sci* 2011;124(Pt 5):755–64.

- Ramdas NM, Shivashankar GV. Cytoskeletal control of nuclear morphology and chromatin organization. *J Mol Biol* 2015;427:695–706.
- Rao L, Perez D, White E. Lamin proteolysis facilitates nuclear events during apoptosis. *J Cell Biol* 1996;135(Pt 1):1441–55.
- Ray P, Chapman SC. Cytoskeletal reorganization drives mesenchymal condensation and regulates downstream molecular signaling. *PLoS One* 2015;10:e0134702.
- Raz V, Carloti F, Vermolen BJ, van der Poel E, Sloos WC, Knaan-Shanzer S, et al. Changes in lamina structure are followed by spatial reorganization of heterochromatic regions in caspase-8-activated human mesenchymal stem cells. *J Cell Sci* 2006;119(Pt 20):4247–56.
- Rezniczek GA, de Pereda JM, Reipert S, Wiche G. Linking integrin alpha6beta4-based cell adhesion to the intermediate filament cytoskeleton: direct interaction between the beta4 subunit and plectin at multiple molecular sites. *J Cell Biol* 1998;141:209–25.
- Schochlin M, Weissinger SE, Brandes AR, Herrmann M, Moller P, Lennner JK. A nuclear circularity-based classifier for diagnostic distinction of desmoplastic from spindle cell melanoma in digitized histological images. *J Pathol Inform* 2014;5:40.
- Schwartz YB, Pirrotta V. A new world of polycombs: unexpected partnerships and emerging functions. *Nat Rev Genet* 2013;14:853–64.
- Sharov AA, Fessing M, Atoyan R, Sharova TY, Haskell-Luevano C, Weiner L, et al. Bone morphogenetic protein (BMP) signaling controls hair pigmentation by means of cross-talk with the melanocortin receptor-1 pathway. *Proc Natl Acad Sci USA* 2005;102:93–8.
- Sharov AA, Li GZ, Palkina TN, Sharova TY, Gilchrest BA, Botchkarev VA. Fas and c-kit are involved in the control of hair follicle melanocyte apoptosis and migration in chemotherapy-induced hair loss. *J Invest Dermatol* 2003;120:27–35.
- Shumaker DK, Dechat T, Kohlmaier A, Adam SA, Bozovsky MR, Erdos MR, et al. Mutant nuclear lamin A leads to progressive alterations of epigenetic control in premature aging. *Proc Natl Acad Sci USA* 2006;103:8703–8.
- Solovei I, Wang AS, Thanisch K, Schmidt CS, Krebs S, Zwerger M, et al. LBR and lamin A/C sequentially tether peripheral heterochromatin and inversely regulate differentiation. *Cell* 2013;152:584–98.
- Sosa BA, Kutay U, Schwartz TU. Structural insights into LINC complexes. *Curr Opin Struct Biol* 2013;23:285–91.
- Srivastava R, Ahn SH. Modifications of RNA polymerase II CTD: connections to the histone code and cellular function. *Biotechnol Adv* 2015;33(Pt 1):856–72.
- Stewart RM, Zubek AE, Rosowski KA, Schreiner SM, Horsley V, King MC. Nuclear-cytoskeletal linkages facilitate cross talk between the nucleus and intercellular adhesions. *J Cell Biol* 2015;209:403–18.
- Troy TC, Turksen K. In vitro characteristics of early epidermal progenitors isolated from keratin 14 (K14)-deficient mice: insights into the role of keratin 17 in mouse keratinocytes. *J Cell Physiol* 1999;180:409–21.
- Truong AB, Kretz M, Ridky TW, Kimmel R, Khavari PA. p63 regulates proliferation and differentiation of developmentally mature keratinocytes. *Genes Dev* 2006;20:3185–97.
- van Kruijsbergen I, Hontelez S, Veenstra GJ. Recruiting polycomb to chromatin. *Int J Biochem Cell Biol* 2015;67:177–87.
- Vergnes L, Peterfy M, Bergo MO, Young SG, Reue K. Lamin B1 is required for mouse development and nuclear integrity. *Proc Natl Acad Sci USA* 2004;101:10428–33.
- Viganò MA, Lamartine J, Testoni B, Merico D, Alotto D, Castagnoli C, et al. New p63 targets in keratinocytes identified by a genome-wide approach. *EMBO J* 2006;25:5105–16.
- Wallace L, Roberts-Thompson L, Reichelt J. Deletion of K1/K10 does not impair epidermal stratification but affects desmosomal structure and nuclear integrity. *J Cell Sci* 2012;125(Pt 7):1750–8.
- Wijchers PJ, Geeven G, Eyres M, Bergsma AJ, Janssen M, Verstegen M, et al. Characterization and dynamics of pericentromere-associated domains in mice. *Genome Res* 2015;25:958–69.
- Wilhelmsen K, Litjens SH, Kuikman I, Tshimbalanga N, Janssen H, van den Bout I, et al. Nesprin-3, a novel outer nuclear membrane protein, associates with the cytoskeletal linker protein plectin. *J Cell Biol* 2005;171:799–810.
- Wilson KL, Foisner R. Lamin-binding proteins. *Cold Spring Harb Perspect Biol* 2010;2:a000554.
- Xue JZ, Funabiki H. Nuclear assembly shaped by microtubule dynamics. *Nucleus* 2014;5:40–6.
- Yang A, Schweitzer R, Sun D, Kaghad M, Walker N, Bronson RT, et al. p63 is essential for regenerative proliferation in limb, craniofacial and epithelial development. *Nature* 1999;398:714–8.
- Yang SH, Chang SY, Yin L, Tu Y, Hu Y, Yoshinaga Y, et al. An absence of both lamin B1 and lamin B2 in keratinocytes has no effect on cell proliferation or the development of skin and hair. *Hum Mol Genet* 2011;20:3537–44.
- Zarnegar BJ, Webster DE, Lopez-Pajares V, Vander Stoep Hunt B, Qu K, Yan KJ, et al. Genomic profiling of a human organotypic model of AEC syndrome reveals ZNF750 as an essential downstream target of mutant TP63. *Am J Hum Genet* 2012;91:435–43.
- Zentner GE, Tesar PJ, Scacheri PC. Epigenetic signatures distinguish multiple classes of enhancers with distinct cellular functions. *Genome Res* 2011;21:1273–83.



This work is licensed under a Creative Commons Attribution 4.0 International License. To view a copy of this license, visit <http://creativecommons.org/licenses/by/4.0/>